CHIRALITY 17:S101–S108 (2005)

Determination of the Absolute Configuration and Solution Conformation of the Antifungal Agents Ketoconazole, Itraconazole, and Miconazole with Vibrational Circular Dichroism

DAVID DUNMIRE,[1] TERESA B. FREEDMAN,[1]* LAURENCE A. NAFIE,[1] CHRISTINE AESCHLIMANN,[2] JOHN G. GERBER,[2] AND JOSEPH GAL[2]

[1]*Department of Chemistry, Syracuse University, Syracuse, New York*
[2]*Division of Clinical Pharmacology and Toxicology, University of Colorado Health Sciences Center, Denver, Colorado*

ABSTRACT The absolute configuration assignments of three antifungal agents, (+)-(2*R*,4*S*)-ketoconazole, (+)-(2*R*,4*S*)-itraconazole (with (*S*)-configuration at the *sec*-butyl group) and (+)-(*S*)-miconazole nitrate have been confirmed by using vibrational circular dichroism (VCD). For these three antifungal drugs, this study also provides evidence for the most abundant conformations of miconazole and for the relative conformations of the azole, dichlorophenyl, and methoxyphenyl groups in ketoconazole and itraconazole, in chloroform solution. *Chirality 17:S101–S108, 2005.*

KEY WORDS: DFT calculation; solution conformation; azoles; CYP inhibitors

Antifungal drugs have assumed a great deal importance in the last 20 years as a result of the increased incidence of mucosal and systemic fungal infections, due primarily to immunosuppression associated with AIDS, organ transplantation, and the increased use of cancer chemotherapy.[1] Among the classes of antifungal drugs, the "azoles" are of great importance because they are orally bioavailable.[2] "Azole" refers to the presence of an imidazole or a triazole moiety in the structures of these drugs. The azole moiety is essential in this class of drugs because the mechanism of antifungal action involves the binding of the azole (*N*3 or *N*4) nitrogen to cytochrome P450 51 (CYP51), the fungal enzyme that catalyzes the 14α-demethylation of lanosterol on the pathway to ergosterol, needed for the fungal cell membrane. This binding results in the inhibition of the enzyme, thereby interfering with fungal viability.[3] Ketoconazole and itraconazole are widely used azole antifungal drugs, and both are available for oral administration.[4,5] Ketoconazole is also used as a topical agent, while itraconazole is available for intravenous dosing. The first azole antifungal drug introduced was miconazole, a drug now used only as a topical agent.[4,5]

Ketoconazole, miconazole, and itraconazole are chiral drugs. Clinically, ketoconazole is used as the racemic mixture of the two cis enantiomers, and the absolute configuration has been assigned[6] via enantioselective synthesis as (+)-2*R*,4*S* and (−)-2*S*,4*R* (Fig. 1). Miconazole is also a racemic mixture, and the absolute configuration was determined via enantioselective synthesis[7] as (+)-*S* and (−)-*R* (Fig. 2). Enantioselectivity in some of the biological actions of ketoconazole[8] and miconazole[7] have been reported.

The substituents on the dioxolane ring in itraconazole are also restricted to the cis configuration (as in ketoconazole), but the presence of the additional stereogenic center in the side-chain *sec*-butyl group doubles the number of possible stereoisomers from two (enantiomers) in ketoconazole to four [two pairs of enantiomers, i.e., two racemates (Fig. 3)], and itraconozole is used clinically as a 1:1 mixture of two diastereomeric racemates. The absolute configuration of itraconazole has been reported in the patent literature[9] as (+)-2*R*,4*S*,*R*, (+)-2*R*,4*S*,*S*, (−)-2*S*,4*R*,*R*, and (−)-2*S*,4*R*,*S* ("2" and "4" refer to the two stereogenic centers in the dioxolane ring, and the remaining configurational descriptor is that of the stereogenic center in the *sec*-butyl group) (Fig. 3). Thus, the two epimers with 2*R*,4*S* configuration at the stereogenic centers of the dioxolane ring are dextrorotatory while the two epimers with 2*S*,4*R* configuration at the dioxolane ring are levorotatory, indicating that the direction of optical rotation in these compounds depends on the configurations at the dioxolane chiral centers and is not greatly influenced by the configuration at the *sec*-butyl group (Fig. 3). We have observed stereoselectivity in some of the actions of itraconazole.[10]

Contract grant sponsors: National Computational Science Alliance, National Institutes of Health; Contract grant numbers: CHE-000025, 5R01 AI4800.
*Correspondence to: Teresa B. Freedman, Department of Chemistry, Syracuse University, Syracuse, NY 13244-4100. E-mail: tbfreedm@syr.edu
Received for publication 20 September 2004; Accepted 19 November 2004
DOI: 10.1002/chir.20120
Published online in Wiley InterScience (www.interscience.wiley.com).

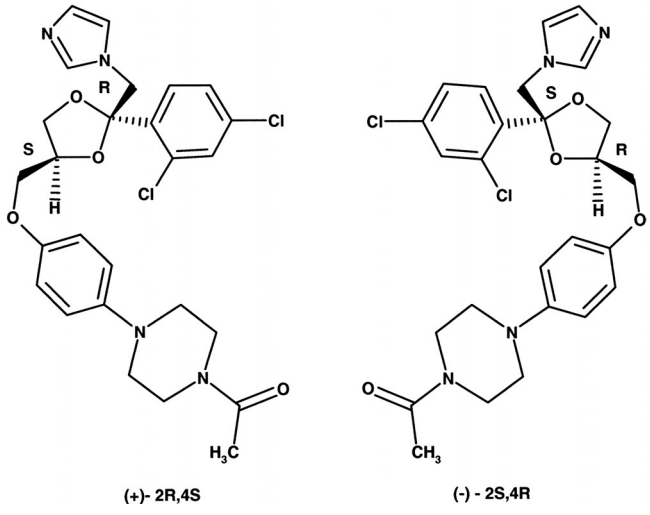

Fig. 1. Enantiomers of ketoconazole.

In view of the considerable current attention paid to the role of stereochemistry in the actions and disposition of chiral drugs,[11] the chirality aspects of the above three azole drugs are of interest. In this communication, we report the results of a study of the absolute configuration and solution conformation of these drugs using vibrational circular dichroism (VCD).

VCD,[12,13] the difference in absorbance of left and right circularly polarized radiation by a chiral molecule during vibrational excitation, is an effective tool for determination of absolute configuration and solution conformation of pharmaceuticals. The technique entails comparison of experimental spectra with calculations on low-energy conformations of a specific enantiomer, carried out at the ab initio or density functional theory (DFT) level.[12,14] Because enantiomers have VCD intensities of opposite sign for each mode, the VCD spectrum provides a unique and rich signature of the absolute configuration. Because of the rapid time scale of vibrational excitation, vibrational spectra are the population-weighted sum of spectra of individual solution conformers. The sensitivity of the vibrational modes to solution conformation and stereochemistry at each chiral center often allows features arising from a specific diastereomer or solution conformer to be identified.

EXPERIMENTAL

(+)-Ketoconazole ((+)-*cis*-1-acetyl-4-[4-[[2-(2,4-dichlorophenyl)-2-(1*H*-imidazol-1-yl)methyl]-1,3-dioxolan-4-yl]methoxyl]phenyl]piperazine, $C_{26}H_{28}N_4O_4Cl_2$) was obtained via semipreparative HPLC resolution of the racemate as described previously.[8] The enantiomeric purity of the isolated compound was >99.9% as determined by analytical HPLC.[8] The dextrorotatory enantiomer was used in the VCD studies.

An analytical HPLC method was first developed for itraconazole.[15,16] The method used a column packed with Chiralcel OD chiral stationary phase (CSP), and two peaks were obtained in the separation. It was shown[15,16] that the less-retained material was the epimeric mixture consisting of the two dextrorotatory diastereoisomers of itraconazole (Fig. 3). Thus, the two stereoisomers that have the 2*R*,4*S* configuration in the dioxolane ring and differing in the configuration at the *sec*-butyl group in the side chain (i.e., (+)-*cis*-(2*R*,4*S*,*RS*) 4-{4-[4-(4-{[2-(2,4-dichlorophenyl)-2-(1*H*-1,2,4-triazol-1-ylmethyl)-1,3-dioxolan-4-yl]methoxy}phenyl)-1-piperazinyl]phenyl}-2,4- dihydro-2-(*sec*-butyl)-3*H*-1,2,4-triazol-3-one) elute as one peak, while the second peak was due to the levorotatory epimeric mixture. The analytical separation was scaled up to a semipreparative HPLC separation by Chiral Tcchnologies, Inc. (Exton, PA), and ~80 mg of the dextrorotatory epimeric mixture was thus obtained. The stereochemical purity of the material (i.e., the percentage of the sum of the two dextrorotatory epimers) was >99.5%, as determined by analytical HPLC on a Chiralcel OD column (4.6 × 50 mm) with a mobile phase of 2-propanol/acetonitrile 90:10 (v/v) delivered at 1.0 ml/min, UV detection at 230 nm. Under these conditions, baseline separation of the two peaks was obtained and the retention times of the two epimeric mixtures were ca. 16 and 20 min, respectively. The dextrorotatory epimeric mixture was used in the VCD studies in the knowledge that the VCD data associated with the *sec*-butyl functionality may be slightly compromised as a result of the partial resolution of the two epimers (see Results and Discussion).

(+)-Miconazole nitrate ((+)-1-(2-(2,4-dichlorophenyl)-2-((2,4-dichlorophenyl)-methoxy)ethyl)-1-imidazole mononitrate, $C_{18}H_{14}N_2OCl_4{\cdot}HNO_3$) was synthesized according the procedure of Godefroi and Heeres.[17] The enantiomeric purity of the product was determined[16] by analytical HPLC as >99.2%. The chromatographic conditions used for this

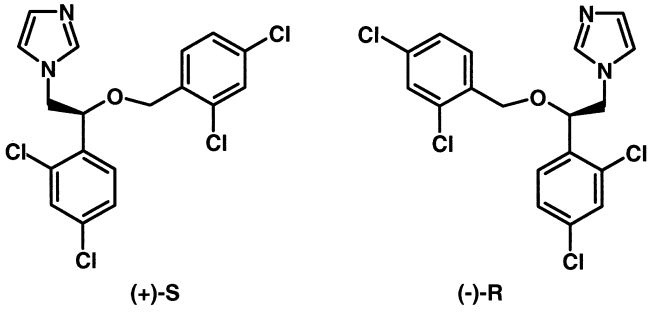

Fig. 2. Enantiomers of miconazole.

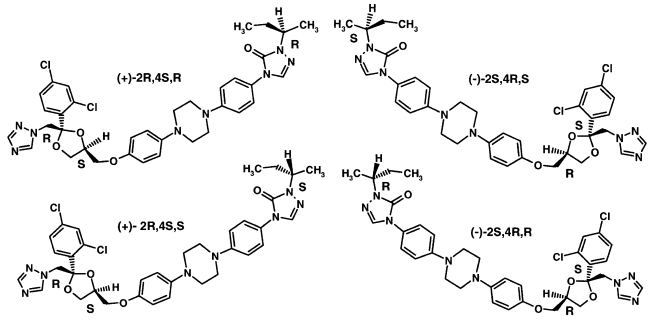

Fig. 3. Four stereoisomers of itraconazole.

analysis included a Chiralpak AD column (Chiral Technologies), with a mobile phase of ethanol/hexane/triethylamine, 95:5:0.1 (v/v/v) delivered at 1.0 ml/min, and UV detection at 244 nm. Under these conditions, the separation factor α = 1.4 and resolution factor R_s = 2.6. The dextrorotatory enantiomer eluted first.

A solution of each compound was prepared with $CDCl_3$ as solvent ((+)-ketoconazole: 6.9 mg/100 μl $CDCl_3$ (0.137 M); (+)-itraconazole: 7.1 mg/100 μl $CDCl_3$ (0.101 M); (+)-miconazole nitrate: 9.4 mg/100 μl $CDCl_3$ (0.203 M)) and placed in a 94.1-μm path length cell with BaF_2 windows. IR and VCD spectra were recorded in the 2000–900 cm^{-1} region on a modified[13] Chiral*IR* FT-VCD spectrometer (BioTools, Inc., Wauconda, IL) at 4 cm^{-1} resolution, with the instrument optimized at 1400 cm^{-1} and with 12 h of collection for sample and solvent.

For identification of solution conformations and confirmation of absolute configuration of (+)-ketoconazole and (+)-itraconazole, a fragment common to the two antifungal agents was used (Fragment 1, Chart 1), selected by truncation of (2*R*,4*S*)-ketoconazole at the 1 position on the phenyl group of the 1-acetyl-4-[4-methoxy(phenyl)]piperazine side chain. The large size and conformational flexibility of these compounds make calculations on the entire structures impractical. Because vibrations of the portion of the ketoconazole side chain excluded in Fragment 1 are unlikely to influence the vibrational modes that involve the two chiral centers on the dioxolane moiety, the calculated spectra of Fragment 1 should provide sufficient characteristic VCD spectral features for comparison to experiment. Several conformers of the (2*R*,4*S*)-configuration of Fragment 1 were optimized with HyperChem (HyperCube Inc., Gainesville, FL) at the semi-empirical PM3 level of theory. The geometries of the lower-energy conformers were further optimized with Gaussian 98,[18] along with calculation of vibrational frequencies and IR and VCD intensities, at the DFT (B3LYP functional/6-31G* basis set) level for the isolated molecule (gas-phase) case. To compare with the experimental spectra, computed frequencies were uniformly scaled by a factor of 0.97 and the intensities were converted to Lorentzian bands with a 6 cm^{-1} half-width at half-height for presentation as Axum 6 plots (Mathsoft Inc., Cambridge, MA). For (+)-itraconazole, Fragment 1 was used to model the chiral centers of the dioxolane moiety, ignoring the differences between the imidazole group of ketoconazole and the triazole group of itraconazole. Calculations on Fragment 2 (Chart 1) were also carried out to assess contributions from the third chiral center in itraconazole. Computational modeling of (*S*)-miconazole was carried out in a similar manner, with the entire molecular structure both for the free base and with the imidazole nitrogen protonated to model the nitrate salt (Chart 1).

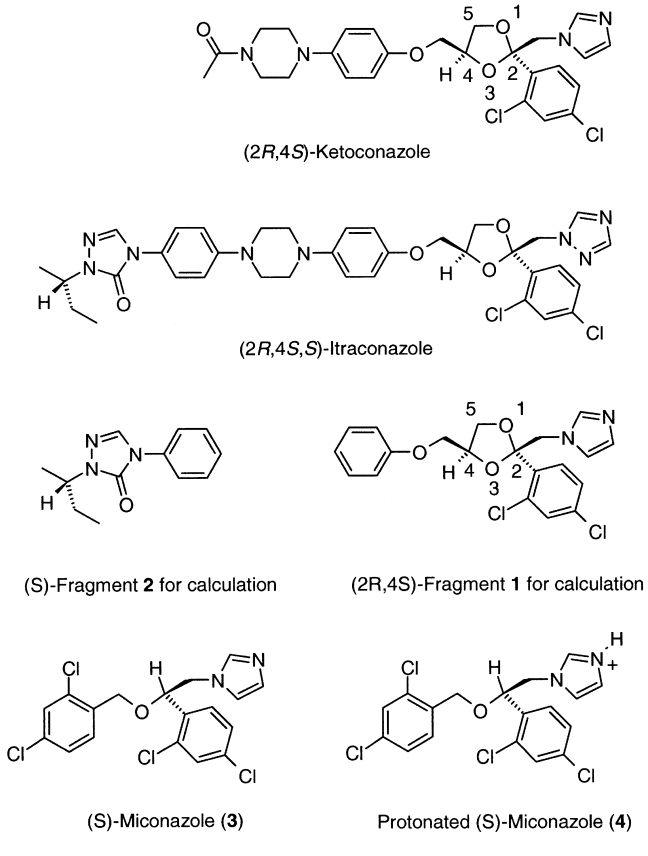

Chart 1

RESULTS AND DISCUSSION

The IR and VCD spectra of the dextrorotatory species of the three antifungal agents are compared in Figure 4. Below 930 cm^{-1}, intense solvent absorbance bands obscure the VCD spectra of the samples. For ketoconazole and itraconazole, the large absorbance at 1510 cm^{-1} (>1.2) introduces high noise in the VCD spectra at that frequency. The VCD spectral patterns for these two compounds are quite similar below 1300 cm^{-1}. A negative VCD feature near 1040 cm^{-1} is common to all three antifungal agents.

The VCD spectra for ketoconazole and itraconazole were first modeled with Fragment 1. The four lowest-energy conformers of Fragment 1 are shown in Figure 5. The (1A, 1B) and (1C, 1D) pairs are generated by 180° rotation of the dichlorophenyl ring, whereas the (1A, 1C) and (1B, 1D) pairs are generated by 180° rotation of the imidazole ring. Rotation of either CH_2R substituent of the dioxolane ring results in conformers 3–5 kcal/mol higher in energy. The IR and VCD spectra calculated for the four low-energy conformers are compared in Figure 6. VCD features 1, 2, 3, 5, 6, and 7 are common to all four conformers, and serve as markers for the (2*R*,4*S*) configuration. Band 1 (1490 cm^{-1}) arises from CH_2 scissors motion, Bands 2 (1208 cm^{-1}) and 3 (1185 cm^{-1}) involve stretch of the dioxolane ring and CH_2 twist, Bands 5 (1031 cm^{-1}) and 6 (~1016 cm^{-1}) arise from dioxolane and imidazole ring stretches, and Band 7 (~956 cm^{-1}) has contributions from three modes involving methylene rock and out-of-plane phenyl hydrogen motion. The sign of feature 4 correlates with the orientation (conformation) of the dichlorophenyl group; Band 4 (1130 cm^{-1}) is generated by

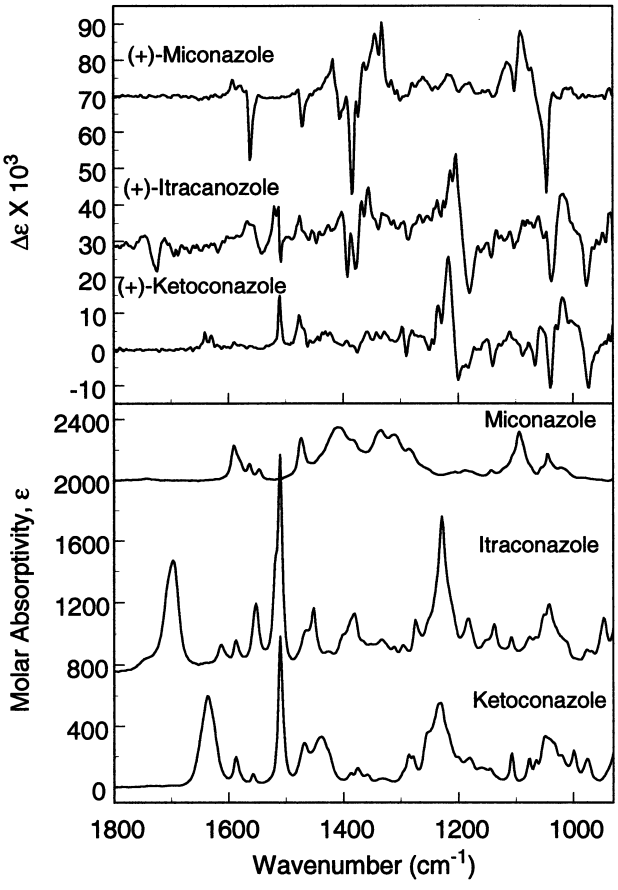

Fig. 4. Comparison of IR (lower frame) and VCD (upper frame) spectra of (+)-ketoconazole (0.137 M), (+)-itraconazole (0.101 M), and (+)-miconazole (0.225 M) in $CDCl_3$ solution, 94.1-μm path length BaF_2, 4 cm^{-1} resolution, 12 h collection for sample and solvent, instrument optimized at 1400 cm^{-1}. Spectra displayed in molar absorptivity units (10^3 cm^2 M^{-1}). Solvent spectra have been subtracted.

methylene rock coupled to in-plane deformation of the dichlorophenyl CH bonds. In Figure 7, the Boltzmann-population-weighted sums of the IR and VCD spectra for the four conformers of Fragment 1 are compared to the experimental spectra for (+)-ketoconazole and (+)-itraconazole. Features 2–7 in the composite calculated VCD spectrum, and a number of additional weak features, correlate well with corresponding features in the observed VCD spectra of the two compounds. This study therefore confirms the (+)-(2*R*,4*S*)-ketoconazole absolute configuration assignment and the assignment (2*R*,4*S*) for the dioxolane ring of (+)-itraconazole. Although itraconazole contains a triazole ring, rather than the imidazole of ketoconazole and Fragment 1, the VCD patterns are quite similar, reflecting the dominant contributions from hydrogen motion throughout the fragment in generating most of the characteristic VCD features. Calculated Band 4 correlates with a negative VCD feature for both compounds, indicating a larger contribution in chloroform solution from the dichlorophenyl orientation in conformers 1A and 1C. Calculated Band 1 is associated with experimental features for which the VCD noise is high because of the high absorbance at 1510 cm^{-1}. The differences between observed and calculated IR spectra arise largely from vibrations of the portion of each molecule that are truncated to generate Fragment 1.

Although the calculated spectra for Fragment 1 provide a good fit to experiment for itraconazole below 1300 cm^{-1}, VCD features between 1350–1400 cm^{-1} and near 1700 cm^{-1} are observed for the (+)-itraconazole sample investigated, but not for (+)-ketoconazole or for the calculations on Fragment 1. Calculations on Fragment 2 in the (*S*)-configuration (Chart 1) were therefore performed to assess

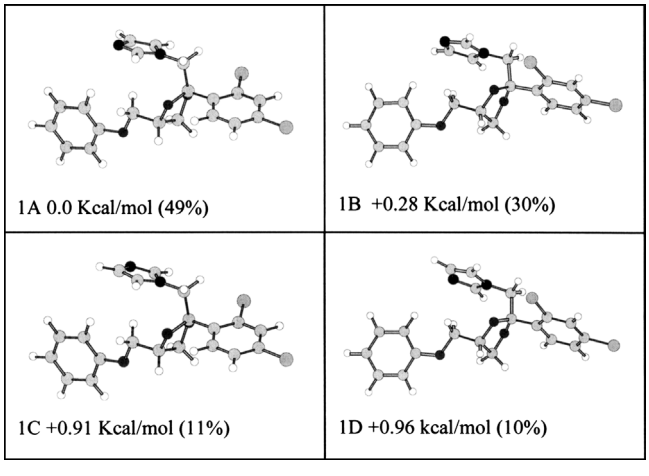

Fig. 5. Optimized low-energy conformers, relative energies, and Boltzmann populations for (2*S*,4*R*)-Fragment 1.

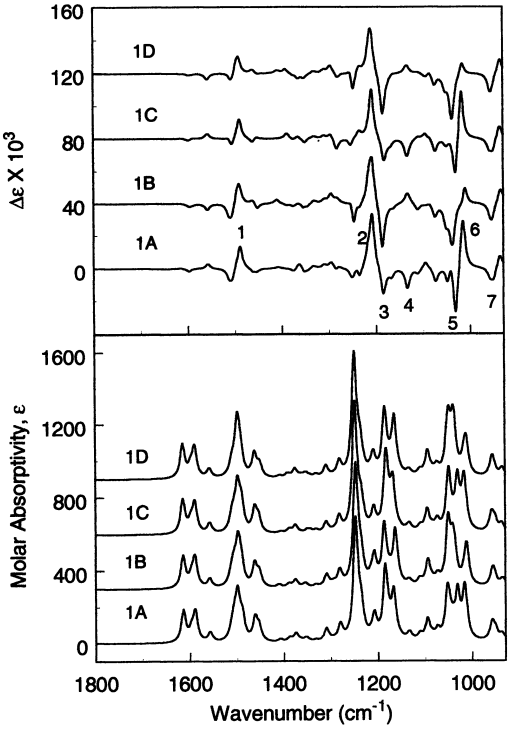

Fig. 6. Calculated IR (lower frame) and VCD (upper frame) spectra for the four lowest-energy conformers of (2*S*,4*R*)-Fragment 1, with spectra offset for clarity. Bands 1–7 serve as markers for configuration and/or conformation.

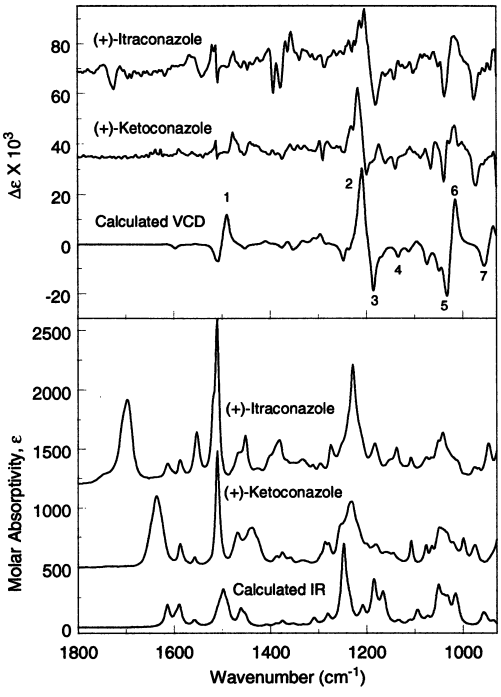

Fig. 7. Comparison of observed IR and VCD spectra of (+)-ketoconazole and (+)-itraconazole with Boltzmann-population-weighted composite calculated spectra for the four lowest-energy conformers of (2*S*,4*R*)-Fragment 1. Spectra displayed in molar absorptivity units, and intensities are offset for clarity.

whether these VCD signals arise from the third chiral center of itraconazole. Four low-energy conformations of Fragment 2 were found, with structures shown in Figure 8 and calculated spectra displayed in Figure 9. Other conformations are 1.5 kcal/mol or more higher in energy compared to 2A. Conformers 2A and 2B differ by the relative orientation of the two rings (+30° and −30° dihedral angle). The carbonyl stretch calculated at 1755 cm^{-1} and ring stretches at 1570 cm^{-1} generate VCD of opposite sign for these two orientations. Conformers 2C and 2D form a similar pair, which differ from 2A and 2B by the conformation of

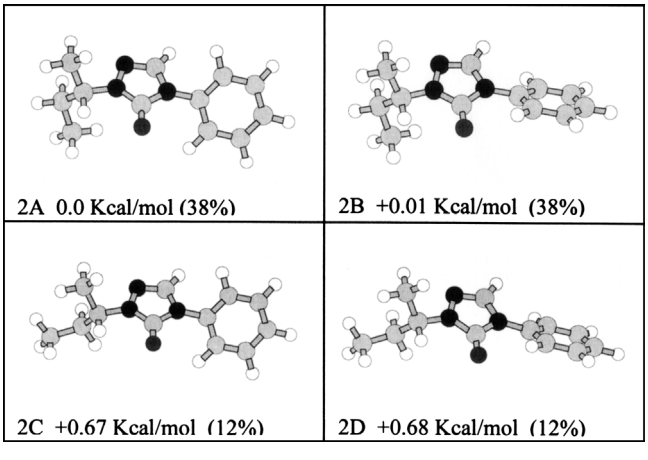

Fig. 8. Optimized low-energy conformers, relative energies, and Boltzmann populations for (*S*)-Fragment 2.

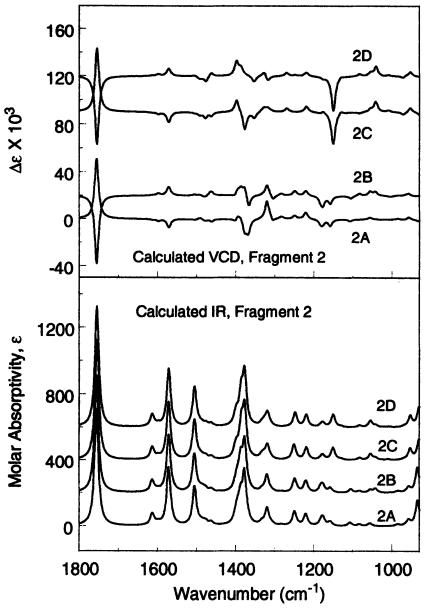

Fig. 9. Calculated IR (lower frame) and VCD (upper frame) spectra for the four lowest-energy conformers of (*S*)-Fragment 2. Spectra offset for clarity.

the (*S*)-*sec*-butyl group. Vibrations of the *sec*-butyl group generate VCD signals of the same sign for each pair of conformers with the same *sec*-butyl conformation. The Boltzmann-population-weighted sum of calculated VCD spectra for the four conformers of Fragment 2 (Fig. 10) display a net weak negative VCD for the carbonyl stretch, and non-zero VCD signals in the 1350–1400 cm^{-1} region

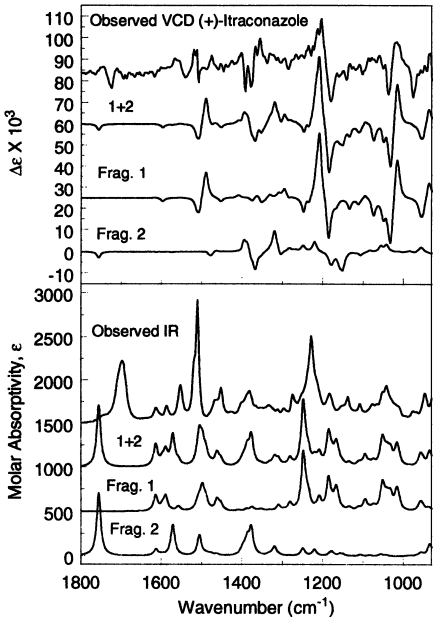

Fig. 10. Comparison of observed IR and VCD spectra of (+)-itraconazole with Boltzmann-population-weighted composite calculated spectra for the four lowest energy conformers of (2*S*,4*R*)-Fragment 1 and (*S*)-Fragment 2, and with the sum of the composite spectra for Fragments 1 and 2. Spectra displayed in molar absorptivity units, and intensities are offset for clarity.

corresponding to *sec*-butyl CH deformations. The sum of the composite spectra calculated for Fragments 1 and 2 show good agreement with the observed IR and VCD spectra of (+)-itraconazole over the entire region investigated (Fig. 10). The comparison of observed and calculated VCD spectra thus support the assignment (2*R*,4*S*) for the absolute configuration of the dioxolane ring and (*S*) for the absolute configuration of the *sec*-butyl substituent in the dextrorotatory sample provided. Because of the large spatial separation between the *sec*-butyl group and the dioxolane chiral centers, and thus only minor interaction between the groups, the presence of equal populations of *sec*-butyl substituents with *S*- and *R*-configurations in the (+)-itraconazole sample would lead to cancellation of VCD signals in the 1350–1400 cm^{-1} region from the two diastereomers, in contrast to the experimental result. The VCD results suggest that the HPLC preparation provided a dextrorotatory sample with excess *S*-configuration at the *sec*-butyl substituent. This may be due to the manner in which the material was collected during the preparative HPLC, inasmuch as collection of the material giving rise to the first peak may have been cut off early in order to avoid contamination from the second peak. If the two epimers in the first peak are even slightly separated, the early cutoff would result in an enrichment of the material in the earlier-eluting epimer.

For miconazole, the DFT calculations were first performed for the entire molecular structure of the free base with (*S*)-configuration at the single chiral center. For the free base, six low-energy conformers were found (3A–3F), with optimized structures and relative energies shown in Figure 11 and calculated spectra displayed in Figure 12 in comparison to the observed spectra. The (3A, 3B), (3C, 3D) and (3E, 3F) pairs are generated by 180° rotation of the imidazole group. Conformers 3C and 3D differ from 3A and 3B by rotation about the O–CH_2 bond. Conformers 3E and 3F differ from 3C and 3D by 90° rotation about the CH_2–dichlorophenyl bond. Other conformations surveyed were >1.5 kcal/mol higher in energy than 3A. Although many of the IR and VCD features of the experimental sample correlate with bands calculated for one or more of the conformers, several experimental IR or VCD features are not reproduced. Because the sample provided was the nitrate salt, the optimized structures 3A–3F were therefore modified by protonation of the imidazole nitrogen and reoptimized (DFT/B3LYP functional/6-31G(d) basis). The resulting optimized geometries and relative energies are shown in Figure 13 for cations 4A–4F, and the calculated spectra compared to experiment in Figure 14. With the exception of 4A and 4B, the optimized conformations were similar with and without protonation. Conformations 3A and 3B were not stable when protonated; the 2,4-dichlorophenymethoxy group rotated to form 4A and 4B as optimized structures. The calculated spectra for conformers 4A–4F show improved agreement with experiment for the IR. Because these calculations were for the isolated cation, and not the ion pair presumably present in the experimental $CDCl_3$ solution, the relative calculated energies are not valid. For that reason, comparison in Figure 15 is between the observed spectra and the Boltzmann-population-weighted composite spectra for the

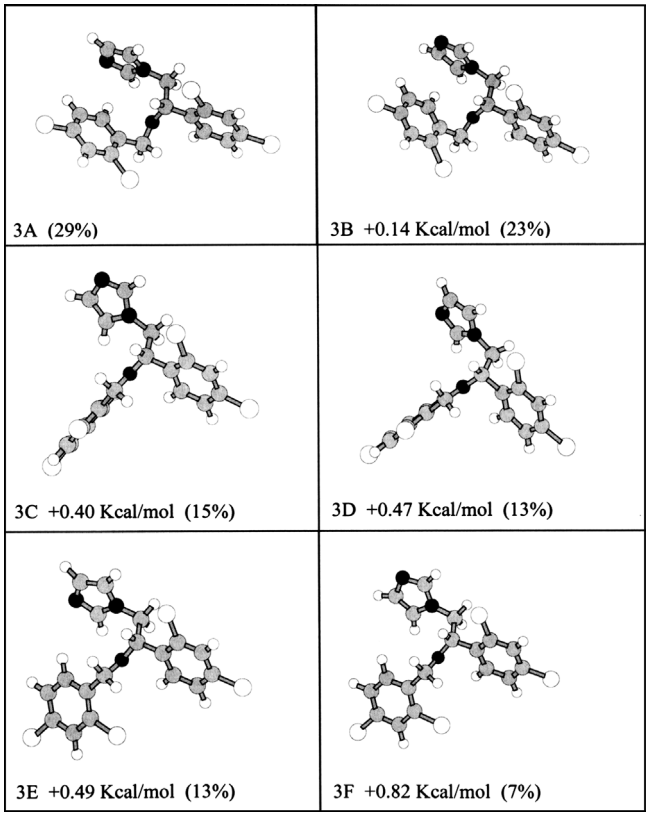

Fig. 11. Optimized low-energy conformers, relative energies, and Boltzmann populations for (*S*)-miconazole free base.

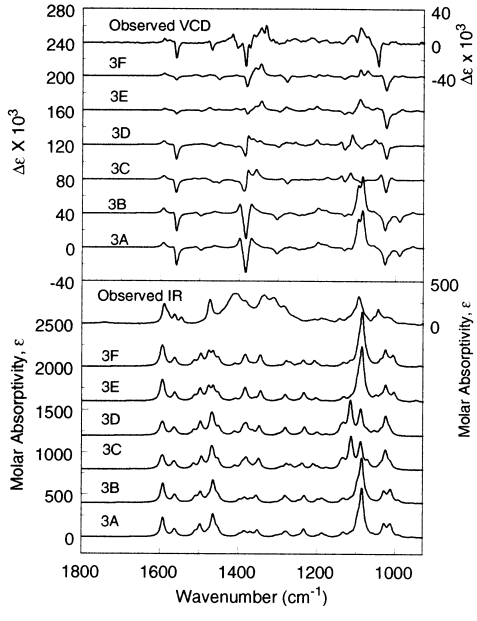

Fig. 12. Calculated IR (lower frame) and VCD (upper frame) spectra for the six lowest energy conformers of (*S*)-miconazole free base (left axes) compared to observed spectra for (+)-miconazole nitrate (right axes). Spectra offset for clarity.

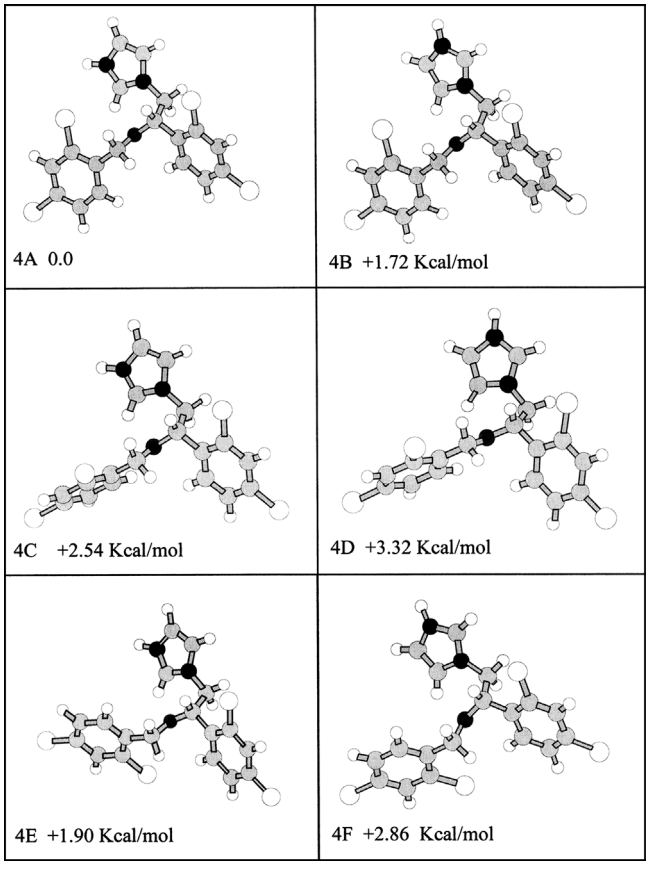

Fig. 13. Optimized low-energy conformers and relative energies for protonated (*S*)-miconazole.

six free-base conformers 3A–3F, and the average spectra for the six protonated conformers 4A–4F. The agreement between experimental and calculated IR and VCD spectra is best for the protonated miconazole average, including the negative VCD feature at 1456 cm^{-1} (calculated)/1471 cm^{-1} (observed) and the IR between 1450 and 1600 cm^{-1}. The excellent agreement between observed and calculated spectra allows assignment of the absolute configuration as (+)-(*S*)-miconazole. The intense broad features in the experimental IR spectrum of miconazole nitrate near 1320 and 1410 cm^{-1} correspond to the antisymmetric NO_3^- stretches in chloroform solution, where the cation and anion would be stabilized by $NH^+ - {}^-ONO_2$ hydrogen bonding with splitting of the degenerate antisymmetric NO_3^- stretch (~1355 for nitrate ion in D_{3h} symmetry). The observed splitting ($\Delta\nu$ ~90 cm^{-1}) can be compared to the splitting measured for phase-IV NH_4NO_3 ($\Delta\nu$ ~125 cm^{-1}),[19] for solid $MgNO_3$ ($\Delta\nu$ ~70 cm^{-1})[20] and for water solvated nitrate ion in chloroform ($\Delta\nu$ ~50 cm^{-1}).[21] For the miconazole solution, VCD is not induced into the NO_3^- modes by the ion pairing.

Comparison of the low-energy miconazole conformers (Figs. 11 and 13) and low-energy Fragment 1 conformers (Fig. 5) reveals a common C(azole)–C–C*–C(dichlorophenyl) dihedral angle near 180° and approximately coparallel planes for the azole and dichlorophenyl substituents

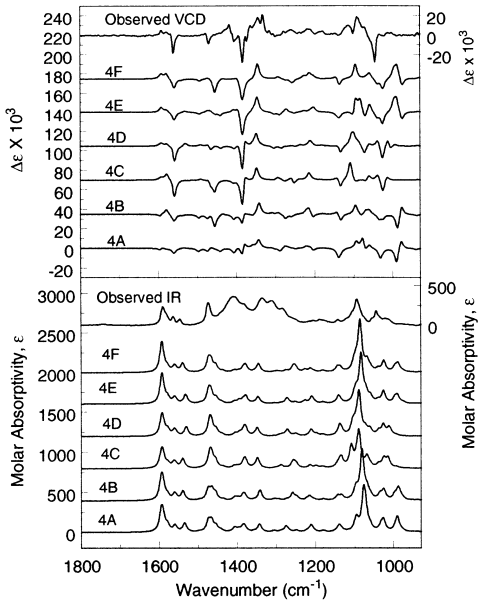

Fig. 14. Calculated IR (lower frame) and VCD (upper frame) spectra for the six lowest energy conformers of protonated (*S*)-miconazole·H^+ (left axes) compared to observed spectra for (+)-miconazole nitrate (right axes). Spectra offset for clarity.

at the same chiral center. These ring orientations are similar to those found for the crystalline fungal agents.[22–25] However, the conformations of the groups at C4 of the dioxolane ring of ketoconazole and itraconazole and of the CH_2–dichlorophenyl group in miconazole differ in the reported crystal structures compared to the low energy conformers identified in this study. Calculations for isolated

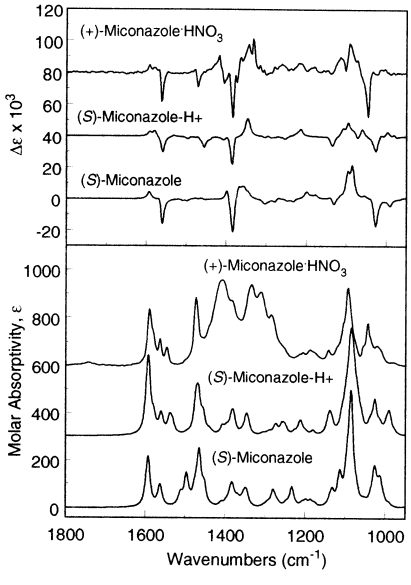

Fig. 15. Comparison of observed IR and VCD spectra of (+)-miconazole with Boltzmann-population-weighted composite calculated spectra for the six lowest-energy conformers of (*S*)-miconazole (free base) and the average spectra for the six conformers of protonated (*S*)-miconazole·H^+. Spectra displayed in molar absorptivity units and intensities are offset for clarity.

Fragment 1 and isolated miconazole with the crystal conformations yield energies much higher than the low-energy conformers reported here, and the calculated VCD spectra for such conformers do not agree with the experimental data for $CDCl_3$ solution.

CONCLUSIONS

For all three antifungal agents, the absolute configuration previously deduced on the basis of synthesis was confirmed with VCD. The VCD assignments are unambiguous, since the opposite enantiomers yield opposite signs for all VCD bands, and comparison to calculations on the trans (2*R*,4*R*)- and (2*S*,4*S*)-diastereomer of Fragment 1 is not necessary because the samples are known to occur in the cis form. In addition, this study has provided information on solution conformations that may be relevant to the mode of action of the drugs.

ACKNOWLEDGMENTS

Supported in part by grant from the National Institutes of Health U.S. Public Health Service (J.G.G. and J.G.). T.B.F. acknowledges partial support of this work from the National Computational Science Alliance, utilizing the University of Kentucky HP SuperDome Complex.

LITERATURE CITED

1. Fisherhoch SP, Hutwagner L. Opportunistic candidiasis—an epidemic of the 1980s. Clin Infect Dis 1995;21:897–904.
2. Como JA, Dismukes WE. Oral azole drugs as systemic antifungal therapy. New Engl J Med 1994;330:263–272.
3. Wrighton AS, Ring BJ. Inhibition of human CYP3A4 catalysed 1′-hydroxy midazolam formation by ketoconazole, nifedipine, erythromycin, cimetidine and nizatidine. Pharm Res 1994;11:921–924.
4. Takashima K, Oki T. Azole antifungal agents. Expert Opin Ther Patients 1996;6:645–654.
5. Nimura K, Niwano Y, Ishiduka S, Fukumoto R. Comparison of in vitro antifungal activities of topical antimycotics launched in the 1990s in Japan. Antimicrob Agents 2001;18:173–178.
6. Rotstein DM, Kertesz DJ, Walker KA, Swinney DC. Stereoisomers of ketoconazole: preparation and biological activity. J Med Chem 1992; 35:2818–2825.
7. Liao YW, Li HX. Enantioselective synthesis and antifungal activity of optically active econazole and miconazole. Acta Pharm Sin 1993; 28:22–27.
8. Dilmaghanian S, Gerber JG, Filler SG, Sanchez A, Gal J. Enantioselectivity of inhibition of cytochrome P450 3A4 (CYP3A4) by ketoconazole: testosterone and methadone as substrates. Chirality 2004;16: 79–85.
9. Heeres J, Mesens JL, Peeters J. Preparation of itraconazole diastereomers. U.S. Patent 5,998,413, December 7, 1999.
10. Gerber JG, Filler SG, Gal J. Stereoselectivity of CYP3A4 inhibition and antifungal activity of the stereoisomers of itraconazole. 6th International ISSX (International Society for the Study of Xenobiotics) Meeting, Munich, Germany, 7–11 October 2001. Abstract 259.
11. Eichelbaum M, Gross AS. Stereochemical aspects of drug action and disposition. Adv Drug Res 1996;28:2–64.
12. Freedman TB, Cao X, Dukor RK, Nafie LA. Absolute configuration determination of chiral molecules in the solution state using vibrational circular dichroism. Chirality 2003;15(9):743–758.
13. Nafie LA. Dual polarization modulation: a real-time, spectral-multiplex separation of circular dichroism from linear birefringence spectral intensities. Appl Spectrosc 2000;54(11):1634–1645.
14. Stephens PJ, Devlin FJ. Determination of the structure of chiral molecules using ab initio vibrational circular dichroism spectroscopy. Chirality 2000;12(4):172–179.
15. Thienpont A, Gal J, Aeschlimann C, Felix G. Studies on stereoselective separations of the "azole" antifungal drugs ketoconazole and itraconazole using HPLC and SFC on silica-based polysaccharides. Analusis Eur J Anal Chem 1999;27:713–718.
16. Gal J, Aeschlimann C, Felix G. HPLC separation of the stereoisomers of ketoconazole, miconazole, and itraconazole on cellulose- and amylose-based chiral stationary phases. 4th International Symposium on Chiral Discrimination, Montreal, Canada, September 19–22, 1993. Abstract 130.
17. Goefroi EF, Heeres J. 1-(β-Arylethyl)imidazoles with fungistatic and bactericidal effects. Ger. Offen. 1,940,388, 26 February 1970.
18. Frisch MJ, Trucks GW, Schlegel HB, Scuseria GE, Robb MA, Cheeseman JR, Zakrzewski VG, Montgomery Jr JA, Stratmann RE, Burant JC, Dapprich S, Millam JM, Daniels AD, Kudin KN, Strain MC, Farkas O, Tomasi J, Barone V, Cossi M, Cammi R, Mennucci B, Pomelli C, Adamo C, Clifford S, Ochterski J, Petersson GA, Ayala PY, Cui Q, Morokuma K, Malick DK, Rabuck AD, Raghavachari K, Foresman JB, Cioslowski J, Ortiz JV, Stefanov BB, Liu G, Liashenko A, Piskorz P, Komaromi I, Gomperts R, Martin RL, Fox DJ, Keith T, Al-Laham MA, Peng CY, Nanayakkara A, Gonzalez C, Challacombe M, Gill PMW, Johnson B, Chen W, Wong MW, Andres JL, Gonzalez C, Head-Gordon M, Replogle ES, Pople JA. Gaussian 98. A.9. Pittsburgh, PA: Gaussian, Inc.; 1998.
19. Tang HC, Torrie BH. Raman study of NH_4NH_3 and ND_4NO_3—250–420 K. J Phys Chem Solids 1977;38:125–138.
20. Waterland MR, Stockwell D, Kelley AM. Symmetry breaking effects in NO_3^-: Raman spectra of nitrate salts and ab initio resonance Raman spectra of nitrate–water complexes. J Chem Phys 2001;114:6249–6258.
21. Davis AR, Macklin JW, Plane RA. Infrared spectroscopic evidence for the solvation of nitrate ion by chloroform and water. J Chem Phys 1969;50:1478–1479.
22. Peeters OM, Blaton NM, De Ranter CJ. *cis*-1-Acetyl-4-(4-{[2-(2,4-dichlorophenyl)-2-(1*H*-1-imidazolylmethyl)-1,3-dioxolan-4-yl]methoxy}phenyl)piperazine: ketoconazole. A crystal structure with disorder. Acta Crystallogr 1979;B35:2461–2464.
23. Peeters OM, Blaton NM, De Ranter CJ. *cis*-2-*sec*-Butyl-4-{4-[4-(4-{[2-(2,4-dichlorophenyl)-2-(1*H*-1,2,4-triazol-1-ylmethyl)-1,3-dioxolan-4-yl]methoxy}phenyl)-1-piperazinyl]phenyl}-2,4-dihydro-3*H*-1,2,4-triazol-3-one (itraconazole). Acta Crystallogr Sect C: Cryst Struct Commun 1996;C52(9):2225–2229.
24. Blaton NM, Peeters OM, De Ranter CJ. The crystal and molecular structure of *trans*-tetrakis(miconazole)cobalt(II) nitrate, $(C_{18}H_{14}Cl_4N_2O)_4Co(NO_3)_2$. Acta Crystallogr Sect B: Struct Crystallogr Cryst Chem 1978;B34(6):1854–1857.
25. Peeters OM, Blaton NM, De Ranter CJ. The crystal structure of 1-{2,4-dichloro-β-[(2,4-dichlorobenzyl)oxy]phenethyl}imidazole hemihydrate: miconazole·1/2 water of hydration. Bull Soc Chim Belg 1979; 88(5):265–272.